BLU-222, a potent and highly selective CDK2 inhibitor, demonstrated antitumor activity as monotherapy and as combination treatment in *CCNE1*-aberrant endometrial cancer models

Nealia House,[1] Victoria Brown,[1] Liang Yuan,[1] Maxine Chen,[1] Stephanie Lee,[1] Rentian Wu,[1] Lakshmi Muthuswamy,[1] Scott Ribich,[1] Philip Ramsden,[1] Kerrie Faia[1]

[1]Blueprint Medicines Corporation, Cambridge, MA, USA

Abstract 1959

Poster available for download at

Background

- *CCNE1* gene amplification and overexpression is associated with chemotherapy resistance and poor survival in many aggressive cancers, including high-grade serous ovarian cancer and endometrial carcinomas (majority of uterine cancers; **Figure 1A and Figure 1B**)[1-4]
- *CCNE1* gene amplification leads to aberrant cyclin-dependent kinase 2 (CDK2) activation, and thereby abnormal retinoblastoma (Rb) phosphorylation and inactivation, and cell cycle checkpoint dysregulation.[1,5] CDK2 is an attractive target for selective inhibition in tumors with *CCNE1* amplification or elevated levels of cyclin E1 (**Figure 2**)
- BLU-222 is a potent, highly selective, orally bioavailable, investigational CDK2 inhibitor (CDK2i) with demonstrated activity as monotherapy and combination treatment in preclinical *CCNE1*-amplified ovarian cancer models, and is currently in early-stage clinical development (NCT05252416)[6,7]
- Herein, we explore additional, specific multivariate biomarkers to predict BLU-222 sensitivity in ovarian and endometrial cancer as monotherapy or in novel combination treatment strategies

Figure 1: *CCNE1*-amplified cancers are CDK2-dependent

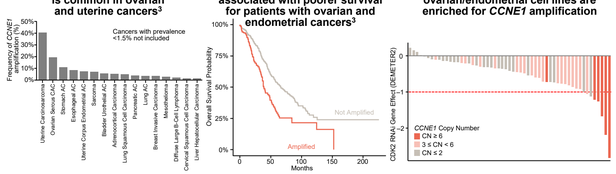

(A) Prevalence of *CCNE1* amplification across several primary tumors and histological subtypes using patient data from TCGA.

(B) Overall survival of patients with ovarian and endometrial cancer with or without *CCNE1* amplification in TCGA.

(C) CDK2 essentiality scores showing RNAi effect (DEMETER2)[8] in ovarian and endometrial cell lines. *CCNE1* CN indicated: amplified, CN ≥ 6, orange bars; gain 3 ≤ CN < 6, light orange bars; normal, CN < 2, gray bars

AC, adenocarcinoma; CAC, cystadenocarcinoma; CDK2, cyclin-dependent kinase 2; CN, copy number; RNAi, RNA interference; TCGA, The Cancer Genome Atlas.

Figure 2: Cell cycle checkpoint dysregulation driven by *CCNE1* gene amplification

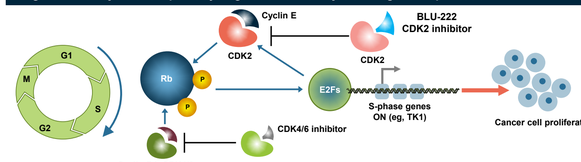

***CCNE1* gene amplification results in aberrant cyclin E levels and CDK2 activation.** Subsequent cell cycle checkpoint dysregulation drives G1/S progression and leads to cancer cell proliferation.

CDK, cyclin-dependent kinase; E2F, elongation factor 2; Rb, retinoblastoma; TK1, thymidine kinase 1.

Results

Figure 3: *CCNE1* amplification sensitized endometrial cell lines to the CDK2 inhibitor BLU-222

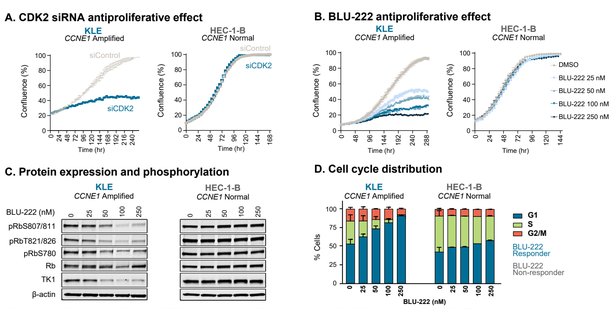

(A) Antiproliferative effect of CDK2 knockdown. Proliferation of *CCNE1*-amplified and *CCNE1*-normal cells transfected with 25 nM CDK2 siRNA or nontargeting siRNA (siControl) was assessed by IncuCyte® cell proliferation assay.

(B) KLE and HEC-1-B cell lines treated with CDK2 inhibitor, BLU-222. Cell proliferation was monitored by IncuCyte® cell proliferation assay.

(C) Pharmacodynamic response to BLU-222. Phospho and total Rb and TK1 expression were evaluated by Western blot in cells treated with increasing concentrations of BLU-222 from 25 to 250 nM.

(D) Cell cycle profile of KLE and HEC-1-B treated with BLU-222. *CCNE1*-amplified (KLE, BLU-222 responder) and *CCNE1*-normal (HEC-1-B, BLU-222 nonresponder) cells were treated with a dose titration of BLU-222 for 24 hours and cell cycle profile determined by Click-iT™ EdU Alexa Fluor™ Flow Cytometry Assay Kit. Error bars represent SEM of at least 2 biological replicates.

CDK2, cyclin-dependent kinase 2; EdU, 5-ethynyl-2'-deoxyuridine; Rb, retinoblastoma; siRNA, small interfering RNA; SEM, standard error of the mean; TK1, thymidine kinase 1.

Figure 4: Whole-genome CRISPR screen identified Rb and p16 loss as markers of resistance to BLU-222 in *CCNE1*-amplified OVCAR-3

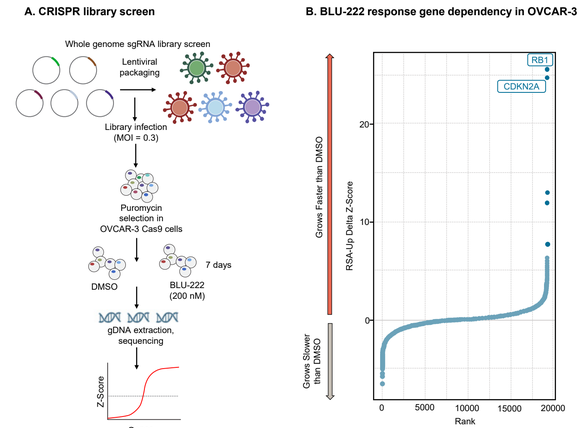

(A) Experimental schematic for assessing gene dependency for response to BLU-222 in OVCAR-3 by CRISPR whole-genome screen. Library transfected cells were treated with BLU-222 (200 nM) for 7 days (Cellecta) and sgRNA abundance was measured in outgrowth cells to calculate gene dependency Z-scores.

(B) Waterfall plot for gene dependencies from CRISPR library screen in BLU-222–treated OVCAR-3. Inactivation of *RB1* and *CDKN2A*, which encode Rb and p16, respectively, were identified as genes whose loss induced resistance to BLU-222.

CDKN2A, cyclin-dependent kinase inhibitor 2A; CRISPR, clustered regularly interspaced short palindromic repeats; DMSO, dimethyl sulfoxide; gDNA, genomic DNA; *RB*/Rb, retinoblastoma gene/protein; sgRNA, single-guide RNA.

Figure 5: Rb and p16 expression predicted response to BLU-222 in cyclin E1-high ovarian and uterine cell lines

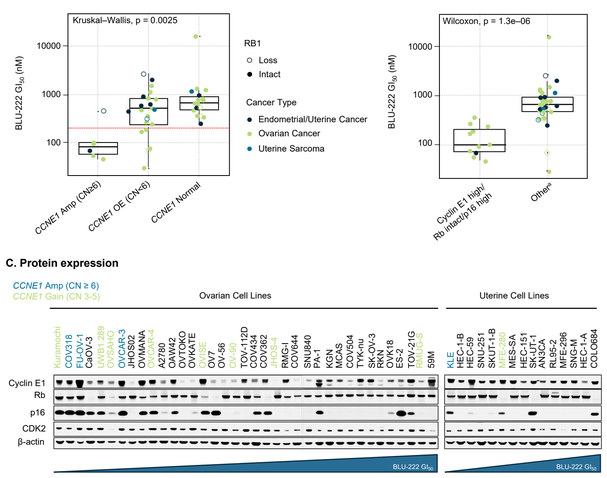

(A) BLU-222 GI_{50} values measured by CyQuant (5d) across a panel of ovarian and uterine cell lines.

(B) BLU-222 GI_{50} in ovarian and endometrial cell lines categorized by the multivariate biomarker signature (cyclin E1 high, Rb-intact, p16 high). Protein expression was derived from Western blot analysis (see Figure 5C). Cyclin E1 high and p16 high were determined based on the distribution of cyclin E1 and p16 across all cell lines. Rb intact was defined as detectable protein and no loss of function mutations.

(C) Protein expression of indicated markers by Western blot in untreated ovarian and uterine cell lines. Cell lines are arranged by their BLU-222 GI_{50} concentrations (left to right, in increasing order).

[a]Other is defined as not meeting criteria for all three biomarkers: cyclin E1 high, Rb intact, and p16 high.
Amp, amplified; CDK2, cyclin-dependent kinase 2; CN, copy number; GI_{50}, concentration for 50% of maximal inhibition of cell proliferation; OE, overexpressing; Rb, retinoblastoma.

Figure 6: BLU-222 monotherapy demonstrated robust antitumor activity in *CCNE1* copy number-increased endometrial PDX models[a]

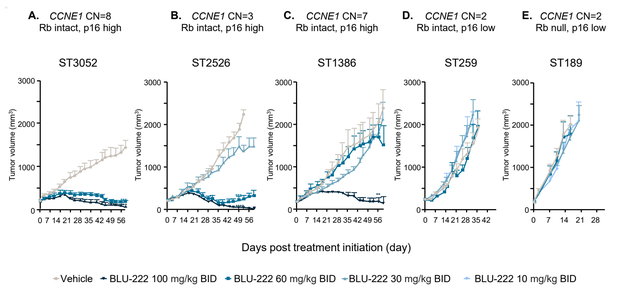

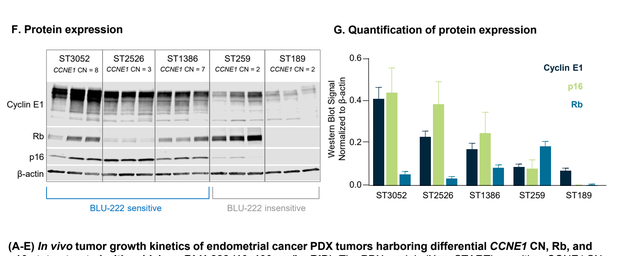

(A-E) *In vivo* tumor growth kinetics of endometrial cancer PDX tumors harboring differential *CCNE1* CN, Rb, and p16 status treated with vehicle or BLU-222 (10–100 mg/kg BID). The PDX models (XenoSTART) are either *CCNE1* CN increased or have high mRNA expression of *CCNE1*. All models were derived from treatment naïve patients except ST2526, which was derived from a patient who had progressed on fluorouracil and radiation. Female mice were implanted with tumor fragments (~70 mg). Treatment was initiated when mean tumor volume reached 150–300 mm^3 and continued through day 60 or when terminal tumor volume was reached (2000 mm^3). Each treatment group contained n=8 mice. Mean tumor volume (mm^3) ± SEM is plotted over time (days). Statistical deviation of treated groups to vehicle is indicated, 2-way ANOVA ** p < 0.01, *** p < 0.001, **** p < 0.0001.

(F) Cyclin E1, Rb, p16, and β-actin protein levels assessed by Western blot in PDX model vehicle tumors.

(G) Cyclin E1, Rb, and p16 Western blot quantifications normalized to β-actin in PDX model vehicle tumors.

[a]Antitumor activity correlates with cyclin E1 high, Rb intact, and p16 high protein levels in endometrial PDX models.
BID, twice a day; CN, copy number; mRNA, messenger RNA; PDX, patient-derived xenograft; Rb, retinoblastoma; SEM, standard error of the mean.

Figure 7: Tumor growth inhibition and BLU-222 exposure correlated to reductions in pRb

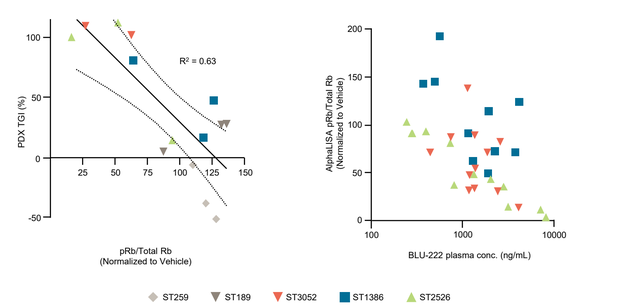

(A) Phosphorylated Rb (pRb)/total Rb signal (AlphaLISA) graphed versus tumor growth inhibition (TGI) of BLU-222 monotherapy in endometrial PDX models.

(B) pRb levels in endometrial cancer PDX tumors treated with BLU-222. pRb was measured using the AlphaLISA SureFire Ultra Detection kit. Y-axis represents the pRb/total Rb ratio, normalized to vehicle across a range of BLU-222 plasma concentrations (X-axis, ng/mL).

CN, copy number; PDX, patient-derived xenograft; PK, pharmacokinetics; Rb, retinoblastoma.

Figure 8: BLU-222 and CDK4/6i ribociclib combination showed an additive effect in uterine cell lines with low p16 expression

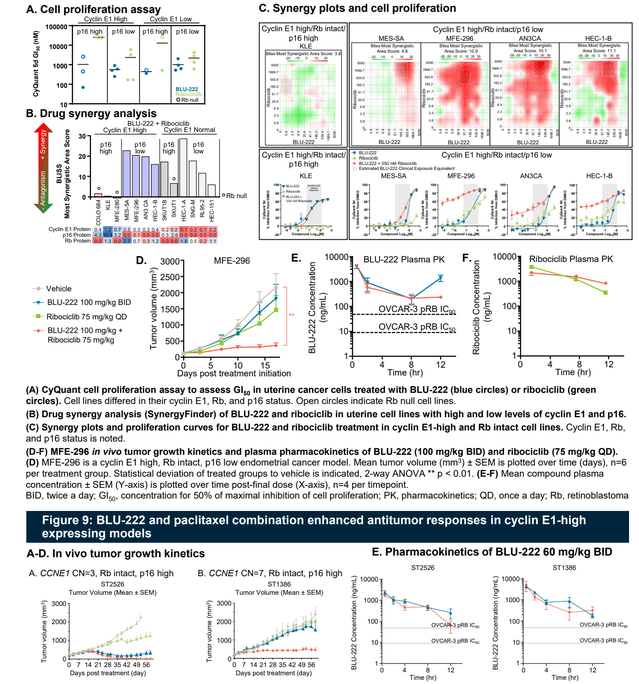

(A) CyQuant cell proliferation assay to assess GI_{50} in uterine cancer cells treated with BLU-222 (blue circles) or ribociclib (green circles). Cell lines differed in their cyclin E1, Rb, and p16 status. Open circles indicate Rb null cell lines.

(B) Drug synergy analysis (SynergyFinder) of BLU-222 and ribociclib in uterine cell lines with high and low levels of cyclin E1 and p16.

(C) Synergy plots and proliferation curves for BLU-222 and ribociclib treatment in cyclin E1-high and Rb intact cell lines. Cyclin E1, Rb, and p16 status is noted.

(D-F) MFE-296 *in vivo* tumor growth kinetics and plasma pharmacokinetics of BLU-222 (100 mg/kg BID) and ribociclib (75 mg/kg QD).
(D) MFE-296 is a cyclin E1 high, Rb intact, p16 low endometrial cancer model. Mean tumor volume (mm^3) ± SEM is plotted over time (days), n=6 per treatment group. Statistical deviation of treated groups to vehicle is indicated, 2-way ANOVA ** p < 0.01. **(E-F)** Mean compound plasma concentration ± SEM (Y-axis) is plotted over time post-final dose (X-axis), n=4 per timepoint.
BID, twice a day; GI_{50}, concentration for 50% of maximal inhibition of cell proliferation; PK, pharmacokinetics; QD, once a day; Rb, retinoblastoma

Figure 9: BLU-222 and paclitaxel combination enhanced antitumor responses in cyclin E1-high expressing models

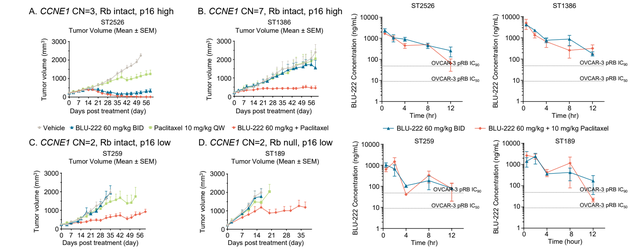

(A-D) *In vivo* tumor growth kinetics of *CCNE1*-aberrant endometrial cancer PDX tumors treated with vehicle, BLU-222 (60 mg/kg BID), and paclitaxel (10 mg/kg QW) either as single agents or combined. The PDX models are either *CCNE1* CN increased or have high mRNA expression of *CCNE1*. Study details are as described in **Figure 6A-E**. Each treatment group contained n=8 mice. Mean tumor volume (mm^3) ± SEM is plotted over time (days).

(E) Pharmacokinetics of BLU-222 as monotherapy (60 mg/kg BID) or in combination with paclitaxel (10 mg/kg) in endometrial cancer PDX tumors with different *CCNE1* CN, Rb, and p16 status. BLU-222 concentration in plasma (ng/mL) (Y-axis) over time post-final dose (X-axis) in respective xenografts. Error bars represent SEM, n=3 or 4 vehicles for each PDX.

BID, twice a day; CN, copy number; IC_{50}, 50% inhibitory concentration; IC_{90}, 90% inhibitory concentration; mRNA, messenger RNA; PDX, patient-derived xenograft; Rb, retinoblastoma; SEM, standard error of the mean; QW, once weekly.

Conclusions

- *CCNE1* amplification predicted CDK2 dependency in ovarian and endometrial cancer cell lines and sensitized these cells to CDK2 inhibition
- In *CCNE1*-amplified endometrial cancer cells, BLU-222, a CDK2 inhibitor, disrupted Rb signaling and resulted in G1 arrest
- BLU-222 demonstrated monotherapy antitumor activity in *CCNE1*-amplified preclinical models of endometrial cancer
- In the cyclin E1-high preclinical models of ovarian and endometrial cancer examined in this study, intact Rb and high p16 provided the optimal context for robust BLU-222 monotherapy activity
- Preclinical *in vitro* and *in vivo* data suggested that BLU-222 in combination with ribociclib may have an additive benefit in *CCNE1*-aberrant endometrial cancers with low p16 expression
- BLU-222 in combination with paclitaxel showed enhanced activity over either single agent in cyclin E1-high endometrial cancer *in vivo* models, regardless of *CCNE1* CN
- These data show that response to CDK2 inhibition by BLU-222 either as single agent or as combination therapy can be further predicted using a multivariate biomarker signature. These data may aid in the interpretation of emerging clinical data in cyclin E1-high tumors and potentially provide rationale for future clinical trial patient selection criteria

References

1. Fagundes R et al. *Front Cell Dev Biol.* 2021;9:774845. 2. Chelmow D et al. *Obstet Gynecol.* 2022;139(4):626–643. 3. National Cancer Institute. The Cancer Genome Atlas program. https://www.cancer.gov/tcga. Accessed January 7, 2022. 4. Gorski JW et al. *Diagnostics (Basel).* 2020;10(5):279. 5. Project Achilles. https://depmap.org/portal/achilles/. Accessed May 10, 2021. 6. Brown V et al. Presented at: AACR Annual Meeting 2022; April 8–13, 2022; New Orleans, LA. Poster 2306. 7. (VELA) Study of BLU-222 in Advanced Solid Tumors. NCT05252416. https://clinicaltrials.gov/ct2/show/NCT05252416. Accessed February 10, 2024. 8. McFarland JM et al. *Nat Commun.* 2018;9:4610.

Acknowledgements and Disclosures

Jian Guo provided DMPK support. The *CCNE1* data across tumor types shown here are in whole or part based upon data generated by The Cancer Genome Atlas (TCGA) Research Network: https://www.cancer.gov/tcga. This research was funded by Blueprint Medicines Corporation, Cambridge, MA. Medical writing and editorial support were provided by Srividya Venkitachalam, PhD, of ProEd Communications, and was supported by Blueprint Medicines Corporation, Cambridge, MA, according to Good Publication Practice guidelines.
NH, LY, MC, SL, RW, LM, SR, PR, and KF are current employees of Blueprint Medicines Corporation. VB was an employee of Blueprint Medicines Corporation at the time the work was conducted.